

International Journal of Hydrology Science and Technology

ISSN online: 2042-7816 - ISSN print: 2042-7808

<https://www.inderscience.com/ijhst>

Probabilistic flood risk assessment using coupled hydrologic and 2D-hydraulic model in the Jhelum River, Northwest Himalayas

Saika Manzoor, Manzoor Ahmad Ahanger

DOI: [10.1504/IJHST.2022.10050494](https://doi.org/10.1504/IJHST.2022.10050494)

Article History:

Received:	25 April 2022
Accepted:	01 August 2022
Published online:	01 December 2023

Probabilistic flood risk assessment using coupled hydrologic and 2D-hydraulic model in the Jhelum River, Northwest Himalayas

Saika Manzoor* and
Manzoor Ahmad Ahanger

Department of Civil Engineering,
National Institute of Technology,
Srinagar, India

Email: saikamanzoor@nitsri.ac.in

Email: manzoorahanger@nitsri.net

*Corresponding author

Abstract: Keeping in mind the susceptibility to flooding-related disasters in the past, the need was identified for flood risk assessment using recent modelling techniques in the data-scarce River Jhelum, India. This study conducted a preliminary rainfall frequency analysis to find the best fit statistical model for calculating peak flow rates for multiple return periods. A framework was followed for the spatio-temporal delineation of flood-prone areas by integrating the watershed modelling system (WMS), Hydrologic Engineering Center-Hydrologic Modelling system (HEC-HMS), and two-dimensional Hydrologic Engineering Center-River Analysis System (2-D HEC-RAS) for different return period design floods. The 2-D unsteady state flood modelling in HEC-RAS showed the river overflowing its flow path for all the return periods, with 55% of the Srinagar city inundated in the 100-year event. The simulated flood depths and velocity maps for every design flood scenario are shown. The 2-D simulations yielded encouraging results compared to the most recent flood event.

Keywords: hydrologic modelling; 2D hydraulic modelling; floodplain delineation; 2D HEC-RAS; River Jhelum.

Reference to this paper should be made as follows: Manzoor, S. and Ahanger, M.A. (2024) 'Probabilistic flood risk assessment using coupled hydrologic and 2D-hydraulic model in the Jhelum River, Northwest Himalayas', *Int. J. Hydrology Science and Technology*, Vol. 17, No. 1, pp.46–74.

Biographical notes: Saika Manzoor is a Senior Research Fellow at the Department of Civil Engineering, National Institute of Technology, Srinagar. She received her BTech in Agricultural Engineering from the Sher-e-Kashmir University of Agricultural Sciences and Technology, Kashmir, India in 2013, and MTech in Soil Water Engineering in 2016. Currently, she is pursuing her PhD in Water Resources Engineering at the Department of Civil Engineering NIT, Srinagar. Her research interests include modern systems of irrigation, climate change studies, hydrological modelling, and integrated water resources management.

Manzoor Ahmad Ahanger holds a PhD in Water Resources Engineering and is currently working as a Professor in the Department of Civil Engineering at the National Institute of Technology, Srinagar, Jammu and Kashmir, India. He has

been working in the areas of hydrology and climate change. He has headed the Department of Civil Engineering, NIT, Srinagar and worked as a Doctoral Program Coordinator and Dean for academic affairs. He has a work experience of more than 30 years at NIT, Srinagar.

1 Introduction

Floods are natural and the most devastating of the catastrophic natural hazards across the globe when the natural channels fill beyond their carrying capacity and inflict damage to rivers, streams, canals, and roadways (Zhang et al., 2014; Nkwunonwo et al., 2020). Frequently produced by extreme heavy events, flashing storm surges, and snowmelt, floods have become a significant concern worldwide, having a tremendous damage potential, most critical for developing countries (Boodhoo, 2003). Rapid storm-event triggered floods destroy farms and infrastructure, disrupt human life and the economy, and eventually lead to epidemics and deaths along the watercourses (Horritt and Bates, 2002; Lee and Lee, 2003; Sharifi et al., 2012; Smith, 2013). The World Health Organization (WHO) reported that more than two billion people were affected by flooding between 1998 and 2017 (Floods, 2019). Some 75% of fatalities arising from floods worldwide have been reported in Asia and South Asia combined (Adhikari et al., 2010). In the 21st century, the research community across the globe has identified a sharp rise in the devastation caused by an increase in the intensity and frequency of floods due to climate change (Xie et al., 2015; Koneti et al., 2018; Thirumurugan and Krishnaveni, 2019; Aryal et al., 2020; Prama et al., 2020). This rise correlates with potential causative factors, including rapid urbanisation, land-use changes, encroachments, poor urban planning, and poor drainage networks (Dawson et al., 2009; UCAR, 2010; Sunkpho and Ootamakorn, 2011; Tabari, 2020).

In this context, the non-structural protective measures used to develop strategies to avert and lessen flood risks and damages include flood modelling methods (Pender and Néelz, 2007; Ghanbarpour et al., 2014). Floodplain modelling with GIS for flood risk communication is increasingly efficient in flood incident management even though such models require extensive data inputs (Derdour et al., 2017; Abdessamed and Abderrazak, 2019). Flood modelling is popular because of the accuracy of its simulations of complex flood flow scenarios and processes. The potential of urban flood risk assessment using integrated flood modelling in developing countries and data-poor areas should invite extensive research for refining region-specific flood models using open source and freely accessible datasets (Nkwunonwo et al., 2020). The increasingly challenging scaling impacts of climate change and urbanisation make it necessary to predict the extent of flooding using refined techniques to safeguard life and assets. Hydraulic models, in this case, play an essential role in the demarcation of flood inundation areas, and 2D models perform better than one-dimensional (1D) models (Quiroga et al., 2017; Liu et al., 2019; Madhuri et al., 2021).

Many studies have been done to map flood-prone areas' vulnerability. To mention a few, (Thakur et al., 2017) conducted a coupled hydrologic and hydraulic modelling using HEC-HMS and HEC-RAS in the USA. (Quiroga et al., 2017) conducted a flood simulation study in Bolivian Amazonia. (Hashemyan et al., 2015) conducted a flood

simulation and inundation assessment in the Khoshke Rudan River, Iran. (Karbasi et al., 2018) conducted a similar analysis for the simulation and flood inundation assessment in Iran. (Thanh Mai and De Smedt, 2017) coupled the hydrologic model-WetSpa and hydraulic model-HEC-RAS for flood prediction in the Huong River, Vietnam. (Kumar et al., 2019) tested the capability of HEC-RAS and global flood monitoring system (GFMS) in Pragyraj, India, for flood risk zone mapping.

Natural hazards are bound to happen, but flood forecasting, installing flood warning systems, and delineating flood-prone areas are needed to safeguard lives and infrastructure. With the extreme events and causative factors of flooding on the rise, the risk of flooding in South Asia and India is disturbing (Steffen et al., 2017; Dottori et al., 2018; Mukherjee et al., 2018). The Himalayan Rivers cause calamitous floods in the contiguous areas and downstream because of extreme monsoonal rainfall events and siltation (Tullos et al., 2016). Considering localised flooding, this also drives attention to the annual loss of forest cover at an unprecedented rate of ~0.45% by constant deforestation and degradation and an increase of around 400% in the settlements in recent times in Kashmir Valley, hinting at enhanced activities and causative factors leading to a leap in the hazardous events (Aasim et al., 2014; Muslim et al., 2014; Wani et al., 2016). Going by the historical records and pieces of evidence, the susceptibility of the state of Jammu and Kashmir, with a population of more than 12 million, to natural disasters is well established and therefore calls for a robust regional planning framework (Shah and Malik, 2017; Romshoo et al., 2018; Shah et al., 2018). The 2014 floods with the highest flow record and long return period in the recent history of Kashmir, were physically driven by strong winds and moisture flux created in J&K, moisture advection from the Arabian Sea, and other synoptic conditions and caused catastrophic damage along the River Jhelum's populated stretches (Ray et al., 2015; Kumar and Acharya, 2016). (Romshoo et al., 2018) state that 853.74 km² of the Jhelum basin was submerged in the 2014 flood period, and (Ahmad et al., 2018) estimate the inundated area in the proximity of Dal Lake to be about 42.50 km² (52.47 % of the total area of the Kashmir Valley). Such events necessitate an assessment of the flood scenario and flood mapping of Srinagar city by demarcating the submerged zones in terms of areal spread, depth, and flow velocity concerning social vulnerability and exposure. This study aimed to assess the risk of flooding under probable critical rainfall scenarios in Srinagar by developing flood inundation maps using the 2D capabilities of HEC-RAS. Identifying flood risk zones based on design storms will enable planning to safeguard lives and minimise damages. This will help guide future city expansion using flood protection strategies based on the vulnerable areas delineated.

1.1 Historical flooding – a concern

The flood records in the Kashmir Valley are usually anecdotal and spurious and lack detailed information about the occurrence of significant flood events. The most recent September 2014 flood [irrigation and flood control (IFC)] brought the city's vulnerable areas to the limelight for careful planning and development. The urbanised flood retention basins raised the bar for vulnerability due to flawed planning systems. From the documentation available, we understand that the following significant events and peak flows occurred in the Kashmir Valley in 1959 (1,302 m³/s), 1966 (1,003 m³/s), 1973 (1,223 m³/s), and 1976 (970 m³/s) (Ballesteros-Cánovas et al., 2020).

1.2 Objectives of the study

The current study covers the following objectives:

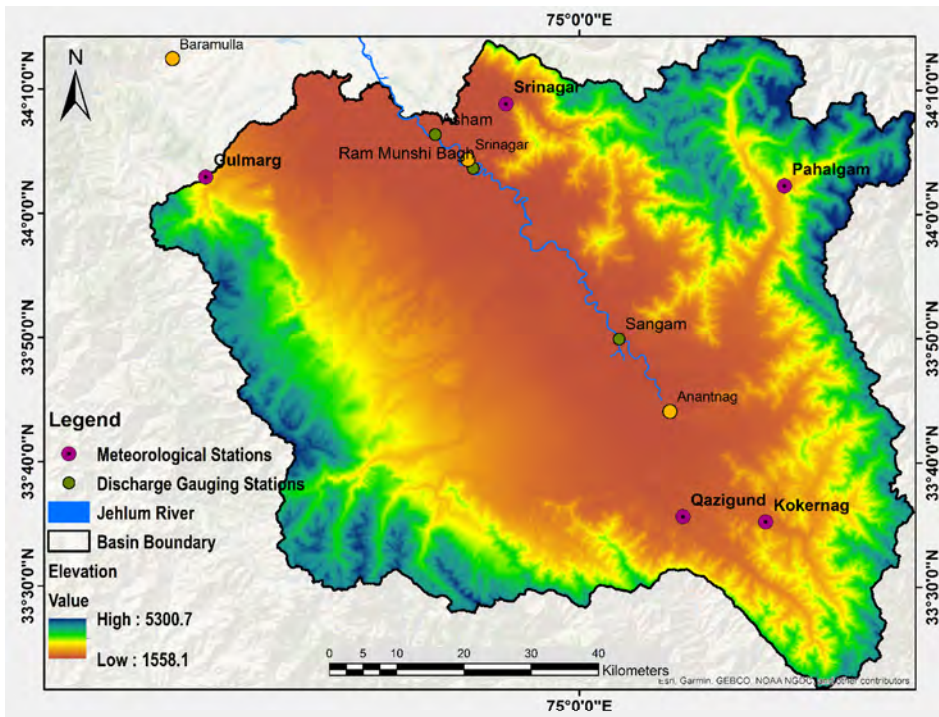
- Hydrological modelling and design flood flow generation for the Srinagar catchment for different recurrence intervals.
- 2D hydraulic modelling for floodplain delineation of the Srinagar City with reference to urban Srinagar.
- Generation of depth, velocity, and flood hazard maps for identifying and marking the flood risk zones.

The authors believe that the methodology followed in the study using relevant and open-source resources is the first for floodplain analysis in the study area and can be updated for application.

2 Data and methodology

2.1 Description of the study area

The union territory of Jammu and Kashmir consists of the southern portion of the larger Kashmir region and is home to several valleys. Among these valleys, the Kashmir Valley is bounded by the Greater Himalayan Range to the northeast and the Pir Panjal Range to the southwest. The perennial tributaries of these ranges (referred to as the right bank and the left bank tributaries, respectively) feed the major tributary of the Indus River system—the Jhelum River, with snow and glacier melt. River Jhelum, the spine of the city's ecology, runs through the valley. The Jhelum, a 129 km long river in the valley, originates from the water of the Verinag Spring (South Kashmir), meanders northwards through alluvium, and crosses the Kashmir Valley to reach Kicchama, Baramullah. Eventually, the river reaches the Indo-Pak border in Uri and flows along the western boundary of the Kashmir valley into Pakistan. The Jhelum, with an average slope of 0.0001 m/m, drains the valley and is joined by the major tributaries at Sangam. The river Jhelum collects and occupies the lowest furrow in the alluvial flat of Kashmir valley (Romshoo et al., 2017). The total length of the Jhelum River is about 725 km (450 miles). The bowl-shaped Kashmir Valley, with an area of 15,220 km² and an elevation ranging between 1,575 to 6,000 masl, is in the Western Himalayan Region, Jammu, and Kashmir, India. With varied topography and geology, the Jhelum basin encompasses the Kashmir valley and covers 47% (17,622 km²) of the valley area. The Jhelum basin (comprising 24 sub-catchments) lies between 33.25° and 34.32° N latitude and 74° to 75.30° E longitude. Figure 1 shows the Srinagar catchment, which was selected for hydrologic modelling and lies between 33°25' and 34°15' N latitude and 74°25' and 75°35' E longitude. It spans an area of about 1,817 km².

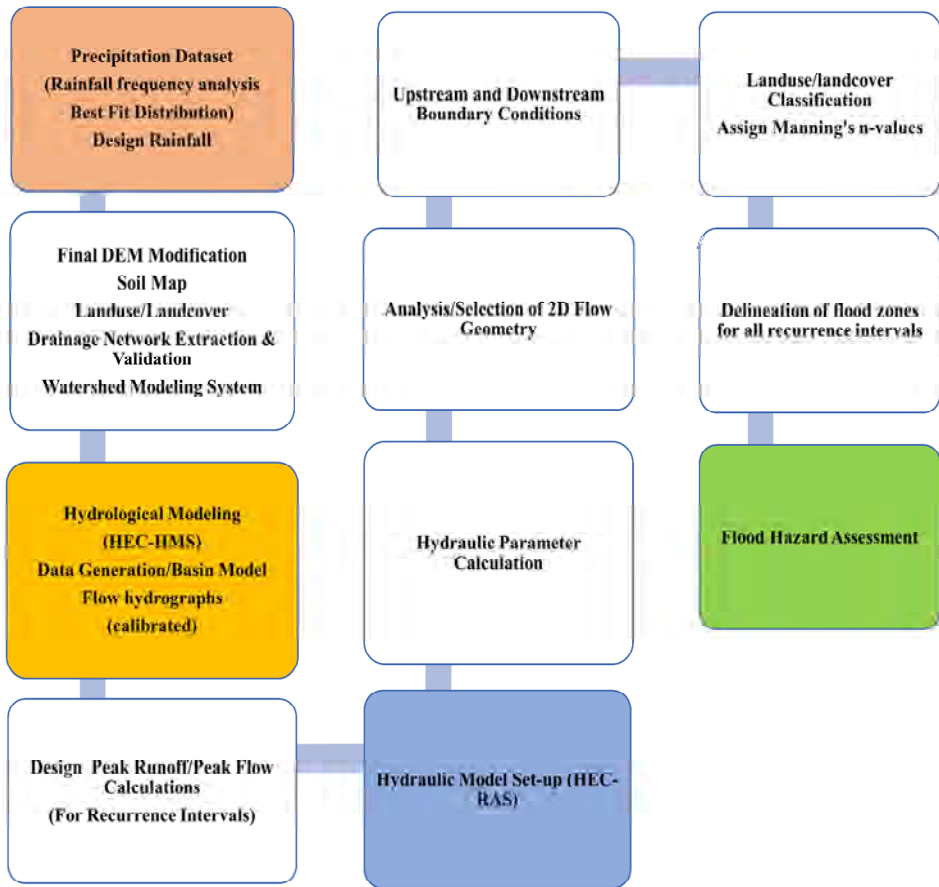
Figure 1 Location of the study area showing the Jhelum River (see online version for colours)

Note: Multi-error-removed improved-terrain (MERIT) digital elevation model used for terrain representation.

Srinagar City and its surrounding areas have an extensive ecological footprint of rivers, streams, lakes, canals, wetlands, forests, hills, gardens, orchards, and agricultural fields. The Anchar, Kushalsar, Dal, and Nigeen are some of the significant lakes, and Hokersar and many smaller wetlands are the regional ecological assets. The low-lying lands in Srinagar city are flood-prone. To avert any adversities due to recurrent flooding, a flood spill channel at Padshahi Bagh allows surplus discharge to drain into Wular Lake – the largest lake for floodwater storage. This flood spill channel carries and diverts the excess discharge to the low-lying areas along the River Jhelum’s eastern bank.

For the temperature and precipitation patterns affected by the relief, the valley of Kashmir experiences the sub-Mediterranean type of climate with four seasons: spring, summer, autumn, and winter. The temperature range is between -5°C and more than 30°C in the Kashmir Valley. The basin’s average annual rainfall is around 693 mm (Ballesteros-Cánovas et al., 2020). Rain plays a critical role in the valley, often raising the chances of flood threats in the valley. Figure 2 shows the research methodology adopted for the integrated flood inundation modelling.

Figure 2 Methodology flowchart for floodplain modelling (see online version for colours)



In this study, data collection, processing of input data, design rainfall calculation, the model set up, the coupled hydrologic and hydraulic modelling, floodplain delineation, and flood hazard mapping are the essential steps discussed to explain the study.

2.2 Modelling software for data analysis

2.2.1 Watershed modelling system (WMS)

The watershed modelling tool, primarily funded by The United States Army Corps of Engineers (COE) and developed by Aquaveo [Environmental Modelling Research Laboratory (EMRL) 2015], is an amalgam of all the watershed solutions. This software application is designed to carry out advanced watershed simulations. WMS 11.0 was used as a pre-processor to determine the watershed geometric data and to develop an input file for hydrological modelling in HEC-HMS 4.9 Beta 10.

2.2.2 HEC-HMS hydrologic model

The Hydrologic Engineering Center-Hydrologic Modelling System (HEC-HMS 4.9 Beta 10) produced by the Hydrologic Engineering Center of the US Army Corps of Engineers (<http://www.hec.usace.army.mil/>) – a comprehensive, semi-distributed, hydrologic modelling tool was used for the study. HEC-HMS works on a three-step model setup that includes preparing the basin model, the meteorological model, and the control specifications for the simulation. The watershed model constructed is used to simulate and analyse peak flows, and later, in HEC-RAS, for floodplain mapping.

2.2.3 HEC-RAS hydraulic model

The Hydrologic Engineering Center-River Analysis System (HEC-RAS) – a windows-based software package is available for 1D and 2D unsteady flow modelling for rivers, flood zone delineation, water surface profile calculations, water quality modelling, and sediment transport calculations (<https://www.hec.usace.army.mil/software/hecras/>). HEC-RAS 6.0 Beta 2 was used for our analysis. It is one of the most capable models for flood risk prediction and visualisation (Alaghmand et al., 2012).

2.3 Watershed data and processing

2.3.1 Hydrometeorological data

Historical daily rain gauge data for the five meteorological stations in the catchment were obtained from the India Meteorological Department (IMD), Srinagar, Jammu and Kashmir. Table 1 lists the nearest meteorological stations in the study area.

Table 1 Meteorological stations used for rainfall frequency analysis

<i>Station</i>	<i>Altitude (m)</i>	<i>Latitude</i>	<i>Longitude</i>	<i>Data availability</i>
Srinagar	1,588	34° 03'	74° 50'	1970–2018
Pahalgam	1,276	34° 02'	75° 20'	1970–2018
Qazigund	1,690	34° 35'	75° 05'	1970–2018
Gulmarg	1,440	34° 03'	74° 24'	1970–2018
Kokernag	1,050	33° 40'	75° 17'	1980–2018

Note: Coordinates are based on datum/projection: WGS-84/UTM Zone 43N.

Table 2 River Jhelum discharge gauging stations

<i>Gauging station</i>	<i>Latitude</i>	<i>Longitude</i>
Sangam	33° 50'	75° 4'
Ram Munshi Bagh	34° 4'	74° 48'
Asham	34° 15'	74° 37'

Table 2 details the discharge gauging stations used for the study. The discharge data were obtained from the planning division, Department of Irrigation and Flood Control (IFC), Kashmir.

2.3.2 Soil, land use, and elevation model data

The harmonised world soil database soil map for the watershed was downloaded from the website <http://www.fao.org/soils-portal/data-hub/soil-maps-and-databases/harmonised-world-soil-database-v12/en/>, processed in Arc Map 10.8, and combined with the land use/land cover data for the curve number calculations. The Srinagar catchment stream network was extracted from the open street maps (OSM) in QGIS (Quantum GIS) software for digital elevation model (DEM) adjustments and corrections. The high-resolution, 10 m land use/land cover data was downloaded from the Environmental Systems Research Institute (Esri) website <https://www.arcgis.com/apps/instant/media/index.html?appid=fc92D38533d440078f17678ebc20e8e2> where a ten class map of land use/landcover has been made available. Derived from the Sentinel-2 source imagery, it provides better accuracy. The Manning's n values from the National Land Cover Dataset (NLCD) were matched for use in HEC-RAS.

Four DEMs: shuttle radar topographic mission (SRTM) –30 m, multi-error removed improved terrain (MERIT) –90 m, NASADEM-30m (modernised DEM data from SRTM), and high resolution ALOS PALSAR –12.5 m (advanced land observing satellite-phased array L-band synthetic aperture radar) were downloaded and checked for vertical elevation terrain representation in the study area. The best suited topographic elevation data, multi-error-removed improved-terrain (MERIT) 90 m DEM (Figure 2), was downloaded from (http://hydro.iis.u-tokyo.ac.jp/~yamadai/MERIT_DEM/) and used to estimate basin characteristics in WMS.

2.3.3 Design rainfall frequency analysis

Probability distributions were used to estimate design rainfall. The data for peak flow calculations were used from the five rain gauges operating in the study. Determining the peak flow according to the repetitive frequency of the extreme rainfall storm (5-year, 10-year, 25-year, 50-year and 100-year) using probability distributions helped assess the hydrological situation considering future extreme events. The annual maximum values were calculated before the design rainstorms were estimated to obtain the flood hydrograph from HEC-HMS. Several probabilistic distribution techniques – Weibull (maximum likelihood), Gamma (maximum likelihood), Pearson Type III (maximum likelihood), GEV (maximum likelihood), Gumbel (maximum likelihood), Exponential (maximum likelihood), Log-Pearson Type 3 were applied to the rainfall data from each station to estimate daily maximum values. The selection of each station's best distribution was based on the goodness of fit of the distribution functions (see supplementary material). The mean precipitation in the station's influence zone was then calculated using Thiessen polygons. The catchment's average areal daily peak rainfall was calculated for all return periods based on the contributions of the selected representative rainfall stations and the averaged design rainfall values for all return periods imported into the hydrologic model for flood hydrograph estimation for use in HEC-RAS.

2.3.4 Land use classification and processing

The raster land use data were processed and mapped in arc map, 10.8 and stored as a shape file after identifying the classes and matching the symbology to the Esri

classification scheme. The land use raster grid was dissolved to reduce the number of land use classes and converted to a polygon feature of nine classes in arc map. Figures 3 and 4 show the land use classification and the proportional land use in the study area, respectively. The ground truth points were matched with the land use classes identified to assess the feature classes accurately. The vast flood plains of the districts of Anantnag, Kulgam, Shopian, Pulwama, Budgam, and Baramullah, through which the left bank tributaries of the Jhelum River travel, are the places of intense agricultural activity. Croplands cover most of the area surrounding the Jhelum River.

Figure 3 Land use classification of the Srinagar catchment (see online version for colours)

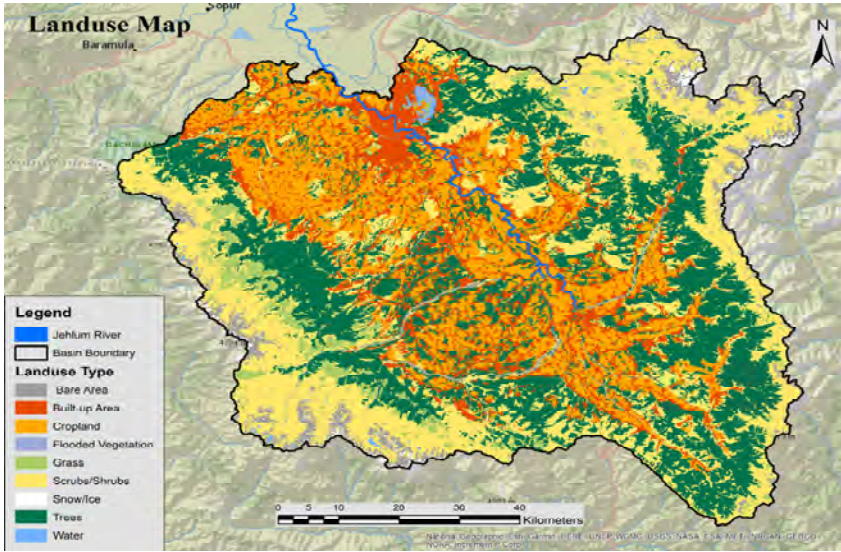
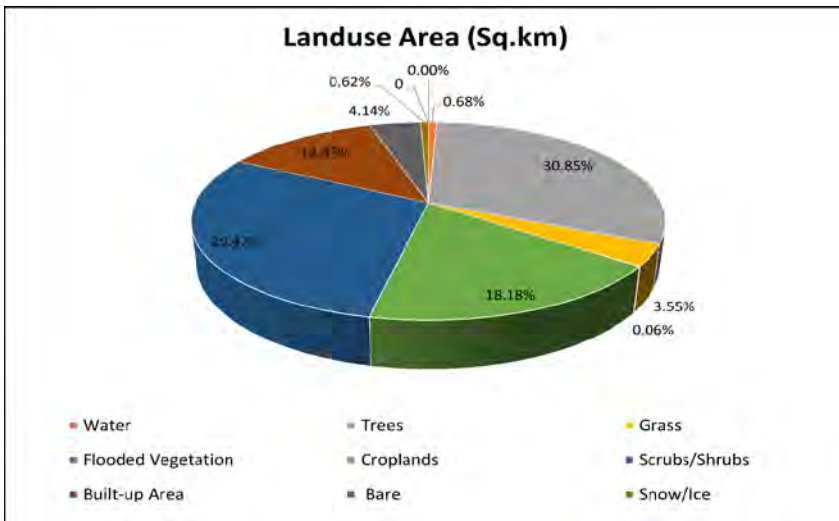


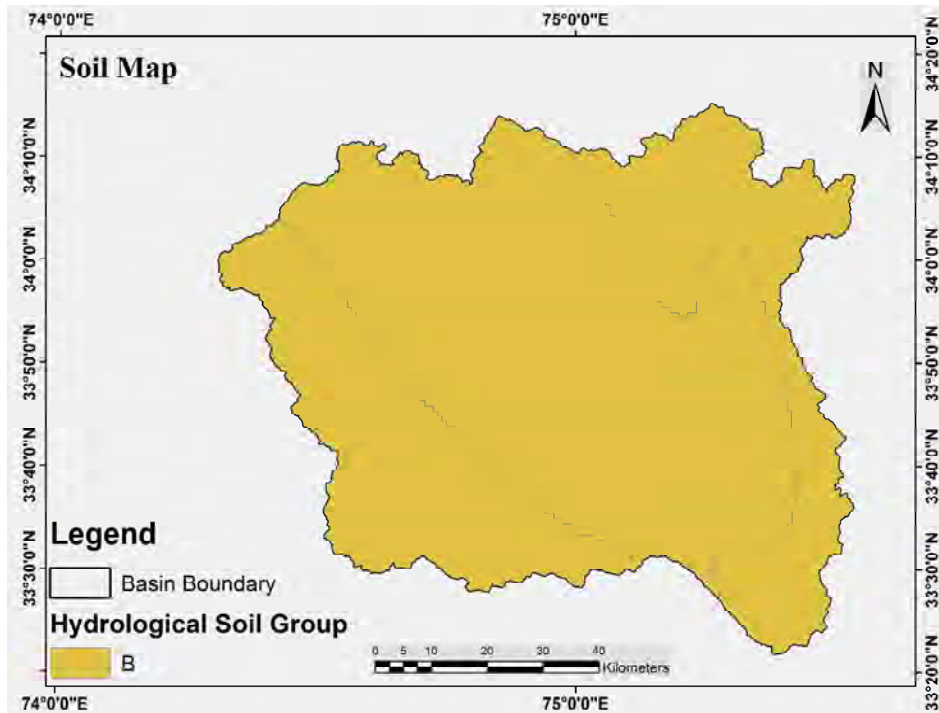
Figure 4 Proportional land use of the Srinagar catchment (see online version for colours)



2.3.5 Soil group classification

The soil map used to estimate the soil infiltration rates, was processed in arc map and combined with the land-use/land-cover data for curve number calculations. By far, the dominant hydrological soil group for the study area was soil code B, as shown in Figure 5. The soil and land-use data were merged to obtain the attributes from the land-use and soil feature classes. After processing the spatial data, the SCS curve numbers available for different land-use and soil group combinations were assigned to create the curve number grid for rainfall infiltration assessment for use in WMS.

Figure 5 Soil map of the Srinagar catchment (see online version for colours)

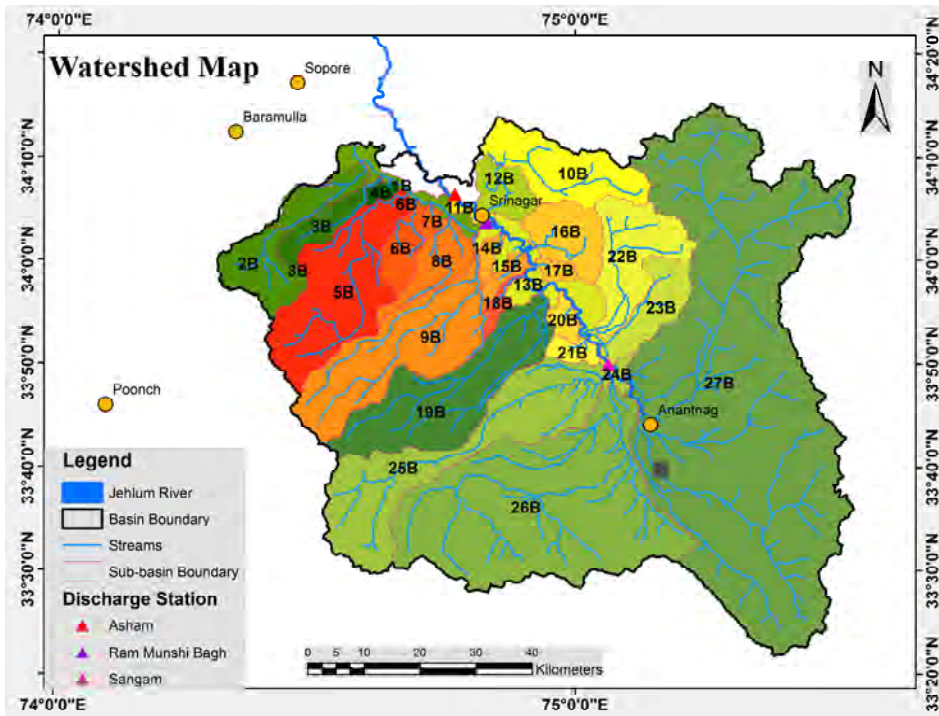


2.3.6 DEM reconditioning

The vertical accuracy of all the DEM's was checked against multiple cross-sections of the River Jhelum by comparing the vertical elevations between selected points with the marked ground reference. The MERIT DEM matched the topography closely and was then georeferenced and processed in WMS for morphometric and hydrologic analysis. The Srinagar catchment's hydrologic modelling boundary was generated based on the meteorological station and the discharge measuring gauge locations. The primary step involved was to analyse the raw DEM for features, which are the mega-river Jhelum, and the stream network connected to it in our catchment. We downloaded the vector data that included a stream network shape file using QGIS by assessing the world imagery and OSM for our study area. Manual corrections were then applied to the DEM to match the street maps and field investigations. The DEM was corrected by a process called burning,

as some streams in the river water network got masked in the raw DEM on initial delineation. Hence, the stream network was given a depth using the drop parameter in the WMS software, so that clear and distinct features of the otherwise missing streams were defined on the reconditioned DEM. WMS software was used to delineate the pre-processed and the reconditioned DEM, and the processed terrain was consistent with the input model stream network fed into WMS to train the streams. This procedure, referred to as terrain pre-processing, was adopted. We aimed to get a drainage pattern after delineation matching the input stream network pattern for use in hydrologic modelling. Table 3 shows the Srinagar basin characteristics after extensive pre-processing and correcting were completed. Figure 6 shows the 27 sub-basins generated in WMS.

Figure 6 Watershed map of the Srinagar catchment with sub-basins (see online version for colours)



Data from the WMS were imported to HEC-HMS to generate the peak discharges for all the return periods. For different return periods and design storms, the soil conservation services-curve number (SCS-CN) method [loss method [equation (1)]] was chosen to estimate the infiltration losses with proper hydrologic routing for obtaining the flow hydrograph of each drainage basin after integrating WMS and HEC-HMS software.

$$P_{ae} = \frac{(P - I_a)^2}{(P - I_a + S)} \tag{1}$$

where

P_{ae} = actual or effective rainfall as direct runoff (mm) at time step t , P = stored rainfall in the catchment (mm) at time step t , I_a = initial abstraction calculated using equation (2).

$$I_a = 0.2S, \tag{2}$$

where

S = maximum potential retention (mm) by the soil calculated using equation (3).

$$S = \frac{25,400}{CN} - 254 \tag{3}$$

where

CN curve number according to the catchment's land use and soil type.

Table 3 Basin characteristics/hydrological parameters of the Srinagar watershed

Basin name	ID	Area (km ²)	Curve number	Basin slope	Max flow distance	Max stream slope	Basin average elevation
1B	1	78.14	69.8	0.02	32,656.3	-0.0004	1,586.4
2B	2	230.6	62.22	0.25	41,508.95	0.05	2,775.3
3B	3	82.33	67.1	0.14	27,874.82	0.02	1,970.3
4B	4	16.14	74.13	0	8,400.06	-0.001	1,582.9
5B	5	426.38	64.77	0.19	61,485.02	0.04	2,630
6B	6	81.18	70.04	0.07	22,677.85	0.009	1,746.6
7B	7	14.84	74.25	0.01	9,197.38	0.0007	1,589.4
8B	8	114.81	72.61	0.05	31,899.18	0.01	1,723.2
9B	9	451.78	63.48	0.18	60,171.19	0.03	2,561.3
10B	10	249.49	59.2	0.43	38,581.74	0.06	2,736.6
11B	11	20.1	88	0.03	16,615.89	0.0014	1,586.2
12B	12	90.92	62.43	0.17	21,337.64	0.0013	1,737.1
13B	13	155.03	65.04	0.1	54,986.32	0.0004	1,674.1
14B	14	23.53	73.64	0	12,761.63	0.0005	1,593.5
15B	15	29.82	72.33	0.01	13,860.58	0.0017	1,600.3
16B	16	143.22	64.56	0.27	18,395.28	0.015	1,944.5
17B	17	23.08	67.79	0.07	9,480.71	0.0006	1,641.7
18B	18	23.78	67.45	0.05	16,282.79	0.0043	1,659.9
19B	19	454.54	64.06	0.13	57,329.23	0.04	2,345.6
20B	20	32.18	69.82	0.01	8,750.53	-0.0003	1,602
21B	21	34.5	69.12	0.02	10,539.81	0.0036	1,627.3
22B	22	238.88	61.18	0.38	38,983.6	0.05	2,597.9
23B	23	133.72	60.65	0.36	24,079.19	0.03	2,215.9
24B	24	21.67	65.58	0.04	8,053.4	0.0008	1,613.6
25B	25	550.63	63.89	0.23	73,443.17	0.03	2,702.6
26B	26	1,114.3	63.46	0.24	80,809.04	0.02	2,481.4
27B	27	2,466.23	60.72	0.39	90,895.06	0.02	2,804

Figure 7 HEC-HMS model of the Srinagar catchment (see online version for colours)

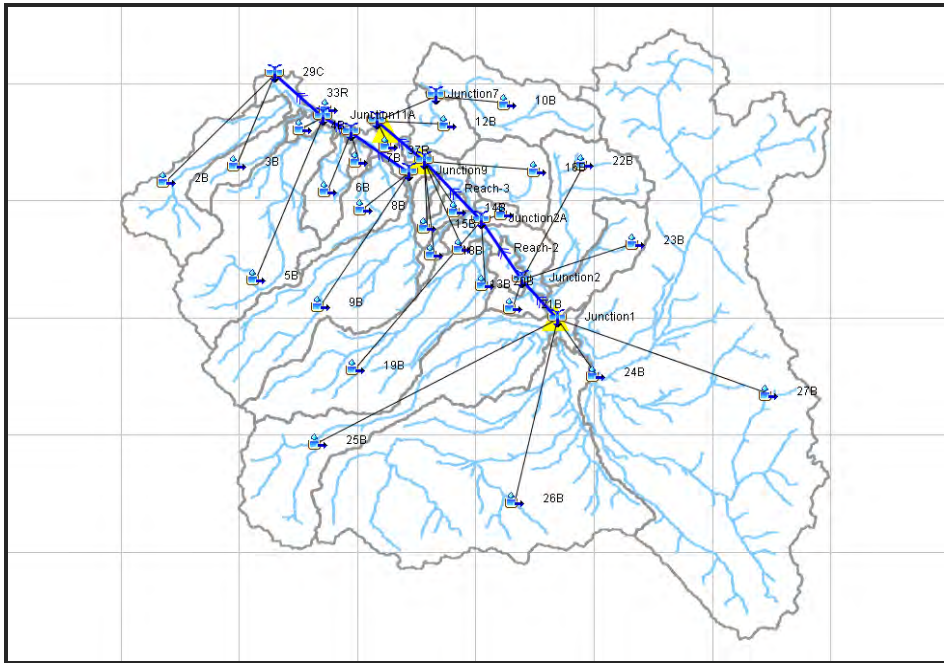


Table 4 Estimated (HEC-HMS) peak flows for different return periods at the main hydrologic junctions

Junctions	Catchment area (km ²)	HEC-HMS peak flow (m ³ /s) by return period (years)				
		5 year	10 year	25 year	50 year	100 year
Junction1 (Sangam)	4,152.84	439.6	1,202.1	1,889.9	2,457.5	3,062.7
Junction10	114.81	51.6	113.8	165.2	205.7	247.5
Junction10A	14.84	9.5	20.6	29.6	36.7	43.9
Junction11	81.18	33.7	79.2	117.8	148.7	180.9
Junction11A (Asham)	426.38	75.2	192.8	297	382.1	472.2
Junction12	16.14	6.7	14.2	20.3	25.1	30
Junction12A	82.33	28.7	73.2	112.2	143.9	177.3
Junction13	230.60	41.6	119.1	190.9	250.6	314.7
Junction2	133.72	27.2	87.8	146.2	195.8	249.3
Junction2A	238.88	39	115.9	188.1	248.5	313.8
Junction3	34.50	13.8	33.3	50	63.4	77.5
Junction3A	32.18	15	35.8	53.6	67.8	82.6
Junction4	454.54	80.4	211.8	329.6	426.2	528.8
Junction4A	23.78	7.8	19.4	29.6	37.8	46.4
Junction5	23.08	14.5	38.3	59.2	76.1	93.7
Junction5A	143.22	51.2	145.9	232.7	304.2	380.1

Table 4 Estimated (HEC-HMS) peak flows for different return periods at the main hydrologic junctions (continued)

Junctions	Catchment area (km ²)	HEC-HMS peak flow (m ³ /s) by return period (years)				
		5 year	10 year	25 year	50 year	100 year
Junction6	29.82	14.3	31.8	46.3	57.8	69.6
Junction6A	23.53	9.6	20.6	29.5	36.5	43.8
Junction7	249.49	44	152.9	260.6	353.3	453.9
Junction8 (Ram Munshi Bagh)	340.41	51.1	170.9	287.6	387.3	495.7
Junction9	451.78	72.5	192.8	301.1	390.3	485.1

The HEC-HMS model was calibrated using the observed peak flow for the 2014 flood event and then validated. The modelled peak flows were in close agreement with the peak discharge data at gauging stations. Figure 7 shows the HEC-HMS basin model for the Srinagar catchment and Table 4 the HEC-HMS generated peak flows for different drainage basins for all return periods.

2.3.7 HEC-RAS SET UP

2.3.7.1 HEC-RAS geometry

The hydraulic modelling was done to determine the hydraulic behaviour and conditions of morphological and developmental changes in Srinagar City and generate flood depths for different return periods. HEC-RAS employs the Saint Venant and Fuzzy Wave equations. The governing continuity and the momentum equations are:

Continuity equation (conservation of mass)

- Conservation form:

$$\frac{\partial Q}{\partial x} + \frac{\partial A}{\partial t} - q = 0 \tag{4}$$

- Non-conservation form:

$$\begin{aligned} \frac{\partial(V_y)}{\partial x} + \frac{\partial y}{\partial t} &= 0 \\ V \frac{\partial y}{\partial x} + y \frac{\partial V}{\partial x} + \frac{\partial y}{\partial t} &= 0 \end{aligned} \tag{5}$$

where V = velocity (m/s), a dependent variable

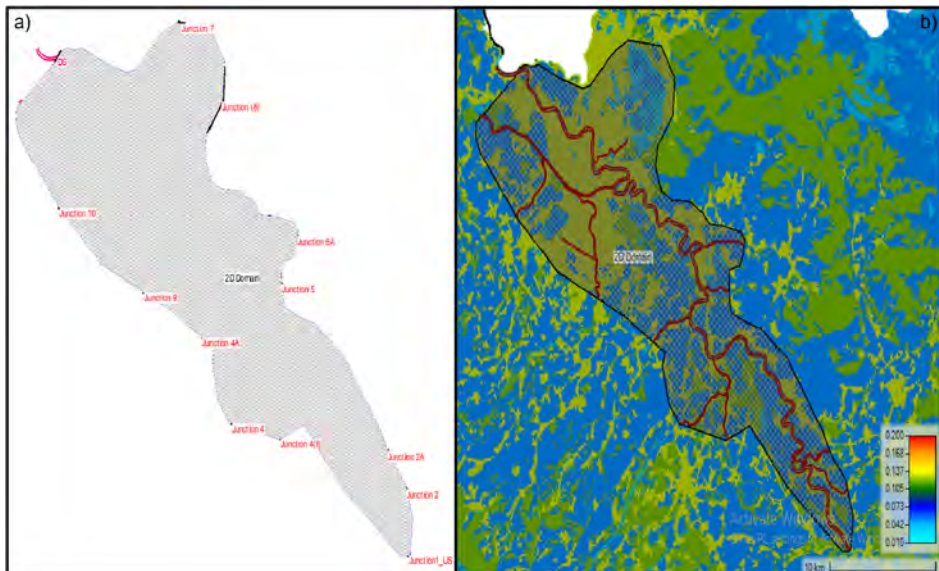
Momentum equation (conservation of momentum):

$$\frac{\partial Q}{\partial t} + \frac{\partial \left(\frac{\beta Q^2}{A} \right)}{\partial x} + gA \left(\frac{\partial y}{\partial x} + S_f + S_e \right) = 0 \tag{6}$$

where Q = discharge through the channel or rate of flow, q = lateral inflow (m/s), x = longitudinal distance alongside channel, t = time, β = momentum correction factor, A = flow cross-section area, V_y = velocity of lateral inflow along y direction, y = water depth(m), S_f = frictional slope, S_e = channel bottom slope due to eddy losses, g = acceleration of gravity.

The 2D flow area was used for detailed floodplain modelling based on the elevation of the Srinagar city on assessing the recent flood layers from the satellite imagery. An Arc GIS processed shapefile was imported for reference. The shape file was used to generate the geometry polygon that included urban Srinagar and those parts of the Srinagar City around the River Jhelum most vulnerable to floods, including all areas below 1,610 masl. The schematic generation of HEC-RAS layers and the methodology followed are mentioned in Figure 2. HEC-RAS was coupled with WMS and HEC-HMS for other data generation. The stream network, the traced mega river rasters, and the land-use map were imported to the HEC-RAS interface. The cross-sections are vital in training the flow to follow the drainage pattern according to the river's capacity. The survey-based 120 cross-sections for the Jhelum River and 16 cross-sections for the flood spill channel obtained from IFC, Srinagar were used to get the footprints of the River Jhelum and the other channels in 2D for HEC-RAS. The cross-sections along with the river centreline from Google Earth images were also used and checked for accuracy with the survey data. An essential task in the model setup was the manual construction of the cross-sections on interpolation wherever unavailable for the rest of the river. The terrain was resampled and then modified according to the channel geometry data at a stage after the 90 m MERIT DEM was eventually reconditioned in GeoTIFF format. Ultimately, the flood flow hydrographs for every recurrence interval were manually entered for the unsteady flow analysis. The flood hydrograph at Junction 1 was used as the upstream boundary condition.

Figure 8 Map showing, (a) 2D flow area and boundary conditions (in red) (b) calculated mesh with land-use map and break lines (see online version for colours)



2.3.7.2 Mesh calculation

The domain of study was divided into relatively small cells (calculation mesh) in HEC-RAS, as shown in Figure 8.

The HEC-RAS computational mesh for the 2D flow area comprised 507,991 cells, with a 40 × 40 m grid used to obtain the hydraulic characteristics of flow. The results were refined manually by removing the faulty or bad cells with more than eight faces from the mesh whenever the grid size was changed, and a run initiated. We checked the model for different cell sizes to obtain satisfactory results and finally set a cell size of 40m resolution. Break lines (cell size of 4 × 4 m) were added for all channels and the Mega River to define flow direction, mark the elevation differences between the channel and the banks in the terrain, and prevent unnecessary flow jumps or leakage. The mesh was revised on every change, and the best results were processed further.

2.3.7.3 Boundary conditions

Boundary conditions were established for all reaches in the 2D flow area of the Jhelum River system. The flow hydrograph data were entered for all boundary conditions, with the normal depth or energy slope (1 in 8,000, source IFC, Srinagar) as the output condition for different peak discharge scenarios considering the unsteady-state flow conditions.

HEC-RAS is structured around the 2D Saint Venant equations, allowing 2D computation to be used and tested for a specific model. After comparing the 2D Saint Venant full momentum results with those from 2D diffusion wave equations, which is the faster and primary default method used in HEC-RAS, not much difference was found. The time-step selection needed consideration and iterations, and the model was run with different time-step choices according to the stability of the model on defining the Courant number. We eventually settled on a computational time interval [time-step (ΔT)] of ten seconds. This was done after tuning the results multiple times by varying the time step from ten minutes to five seconds until a Courant number of less than one was obtained, indicating model stability. The model was run from the higher time step to check the flow behaviour.

2.3.7.4 Manning’s values

Roughness coefficients (Manning’s n) were assigned for each land use/land cover polygon category for the basin grid cells based on defined NLCD values. The land use layers and corresponding values of n were used in the model until the model’s calibrated values were obtained after several successive iterations. Table 5 shows the calibrated values of Manning’s n .

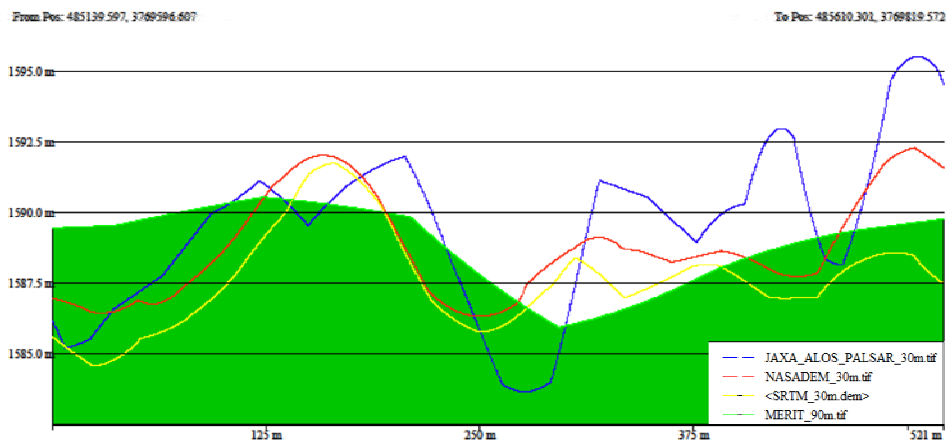
Table 5 Calibrated values of Manning’s n according to land use

Land use type	Built-up area	Flooded vegetation	Water	Trees	Grass	Snow/ice	Crops	Scrubs/shrubs	Bare ground
Manning’s n	0.12	0.04	0.031	0.12	0.04	0.035	0.05	0.05	0.03

3 Results and discussion

The MERIT DEM was selected for analysis based on comparison of the cross-sectional profile analysis, as shown in Figure 9.

Figure 9 Cross-sectional profile of the River Jhelum for DEM comparison (see online version for colours)



Rainfall data from all five stations were evaluated by the probabilistic statistical distribution to obtain the best prediction model for annual maximum daily rainfall for each return period. The goodness of fit was determined to find the best fit distribution for each station among the seven distributions tested. The exponential distribution was found to be the best fit distribution for Srinagar and Pahalgam stations, and the Gumbel distribution was the best for others, as recorded in Table 6.

Table 6 Predicted annual maximum rainfall (mm) for different return periods at all the stations and the best-fit probability distribution

Station	Best fit probability distribution						Best probability distribution (mm/day)
	Return period (years)						
	2	5	10	25	50	100	
Srinagar	51.9	63.1	96.5	122	141	160	Exponential
Pahalgam	61.1	90.9	113	143	166	188	Exponential
Qazigund	89.7	120	141	167	186	205	Gumbel
Gulmarg	89.7	120	141	167	186	205	Gumbel
Kokernag	66	91.1	108	129	144	160	Gumbel

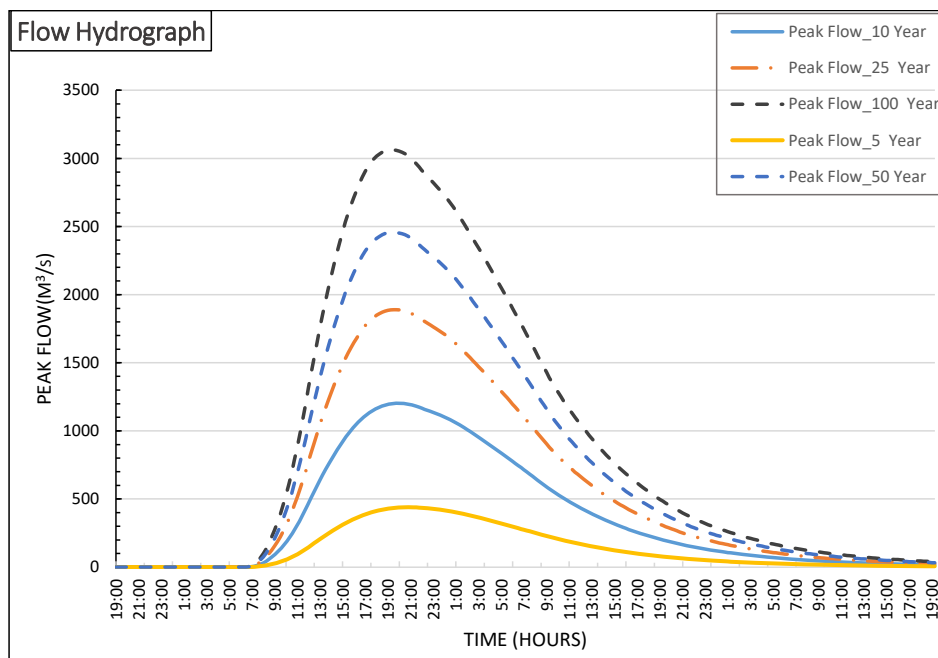
Table 7 shows the Srinagar catchment’s average areal rainfall. The estimated average areal rainfall for the 100-year flood is 159.66 mm. The rainfall for the 2-year and 5-year return periods can be used to plan and design a drainage system. The average areal rainfall was used to determine each return period’s peak flow. The analysis shows that extreme rainfall events are in the range of 60 to 160 mm/day, as per the period of available rainfall data.

Table 7 Average areal daily rainfall (in mm) for the Srinagar catchment

Station name	Return period (in years)						Extreme Rainfall (in mm/day)
	2	5	10	25	50	100	
Srinagar	10.35	1.25	19.25	24.33	28.12	31.91	
Pahalgam	11.63	17.30	21.51	27.22	31.60	35.79	
Qazigund	13.04	17.44	20.50	24.28	27.04	29.80	
Gulmarg	17.01	22.76	26.74	31.67	35.28	38.88	
Kokernag	9.59	13.24	15.70	18.75	20.93	23.26	
Average areal rainfall	61.64	72.02	103.71	126.27	142.99	159.66	

Figure 9 shows the estimated 15-minute hydrographs for the different return periods according to the catchment’s soil, land use, terrain, and other hydrological characteristics, assessed at Junction 1. The peak flows estimated in HEC-HMS for the 100-year extreme event (see Figure10) agreed with the recorded, i.e., actual peak flows. A flow of 3,262 m³/sec was recorded at the Sangam station in the 2014 flood event. The design flood results are close to those of (Bhat et al., 2019), who stated that the flood levels during the 2014 event were higher than most of the known floods recorded, even though the authors conducted 1D steady-state analysis. The peak flow results for the 2-year, 5-year, 10-year, 25-year and 100-year return periods are shown in Table 4. The data from the calibrated HEC-HMS were imported into HEC-RAS for flood flow and hazard analysis and produced quite reliable results.

Figure 10 Hydrograph for Junction 1 (Sangam) for 5-year, 10-year, 25-year, 50-year and 100-year return periods (see online version for colours)



The 2D HEC-RAS boundary [see Figure 8(a)] included the high and medium flood-risk areas below 1,610 masl. The model ran successfully, and the areal extent and velocity floodplain maps were generated. The probable results on the 100-year return period maps are consistent with the areal extent of the actual flood maps of the 2014 flood event from IFC, Srinagar, and the satellite imagery. The MERIT DEM is the best suited for the mountain topography even though it requires reconditioning, but satisfactory results marking the spatial extent of the floods have been observed.

Figure 11 Design flood depth and areal extent of the 100-year flood along the River Jhelum (see online version for colours)

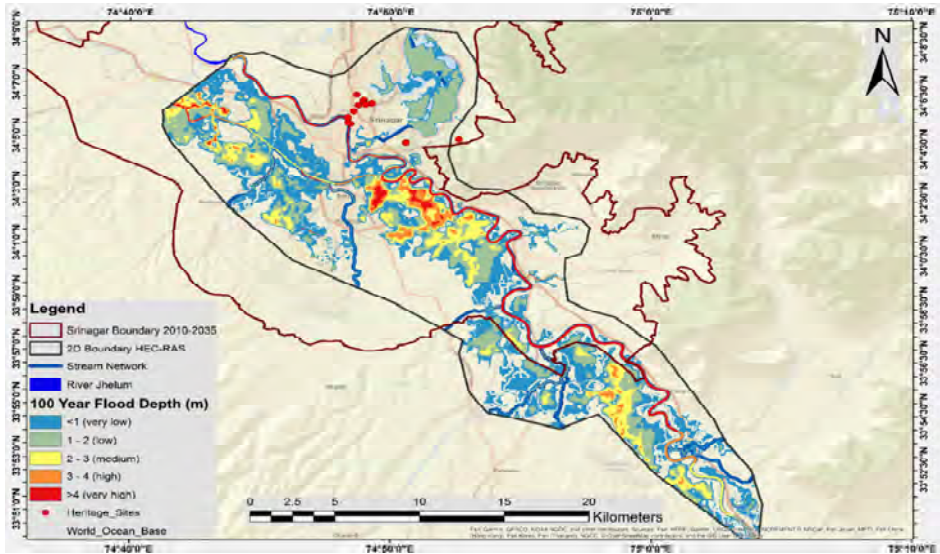


Figure 11 shows the predicted 100-year flood depth. About 55% of the city, including the significant parts of Srinagar, is likely to be inundated if such an extreme event occurs. The very high-risk zones are classified and marked in red in Figure 11, and all the other inundation maps developed for 100-year, 50-year, 25-year, and 10-year floods, as shown in Figures 12, 13, and 14, respectively. The model calibration using the computation time interval and Manning's n was effective in refining the results. Overland flow is observed from Sangam to Srinagar, in general, with Srinagar's flat, bowl-like shape giving rise to some very high-risk zones. The flood spill channel and the main river are inefficient in carrying peak flows, with water depths exceeding 4m in and around the river watercourse and downstream in Srinagar. If strict measures are not taken to improve the situation, disastrous events are inevitable because of rapid development and the wetlands' shrinking to absorb the floodwaters. It is to be noted that even the 10-year design floods may lead to the inundation of many areas of the valley along the River Jhelum due to drainage system failure, as shown in Figure 13. The design flood flow velocities in the study area are shown in Figures 14, 15, 16, and 17 for the 100-year, 50-year, 25-year, and 10-year floods, respectively. Flood flow velocity is between 0.5 to 1 m/s and exceeds 4m/s in the river and many parts of the study area. The risk of the heritage sites falling in the study is also shown in each recurrence interval's flood depth and velocity map. Three heritage sites close to the Jhelum River fall in the very high-risk zone of the 100-year flood event, as shown in Figure 11.

Figure 12 Design flood depth and areal extent of the 50-year flood along the River Jhelum (see online version for colours)

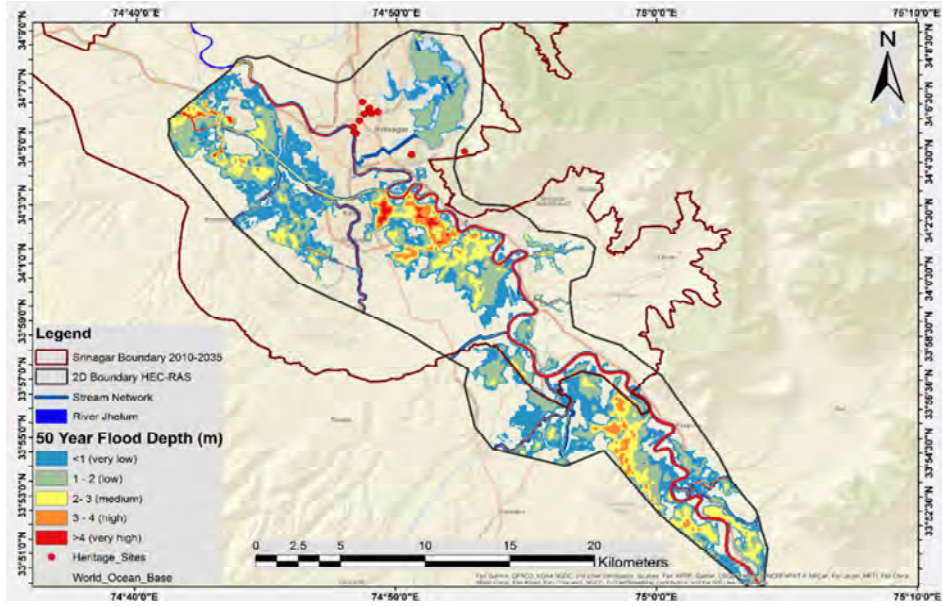


Figure 13 Design flood depth and areal extent of the 25-year flood along the River Jhelum (see online version for colours)

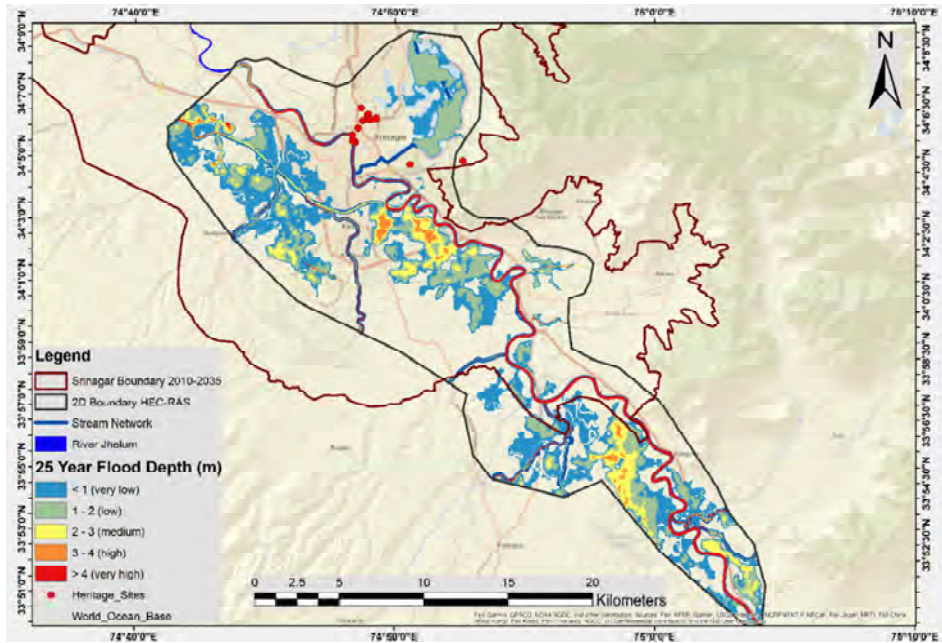


Figure 14 Design flood depth and areal extent of the 10-year flood along the River Jhelum (see online version for colours)

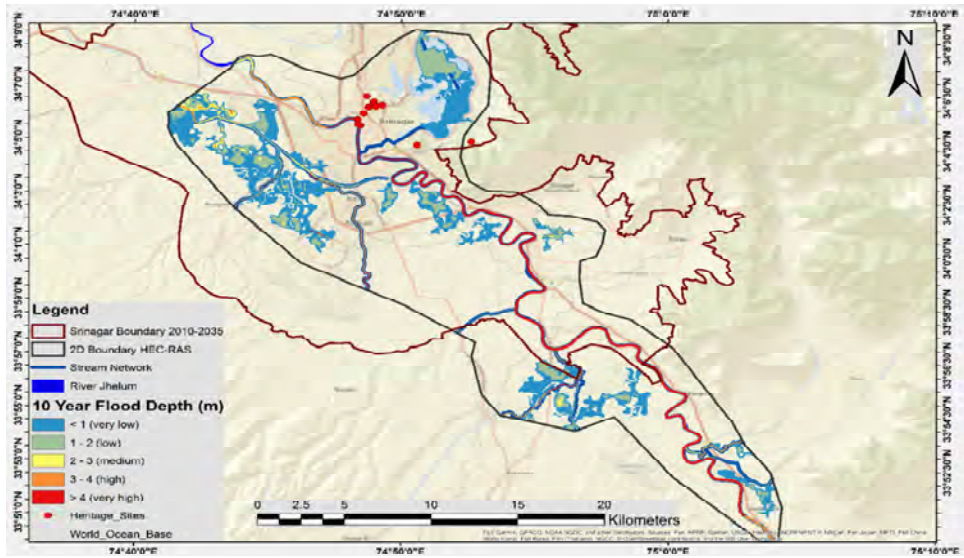


Figure 15 Maximum flow velocity of the 100-year flood (see online version for colours)

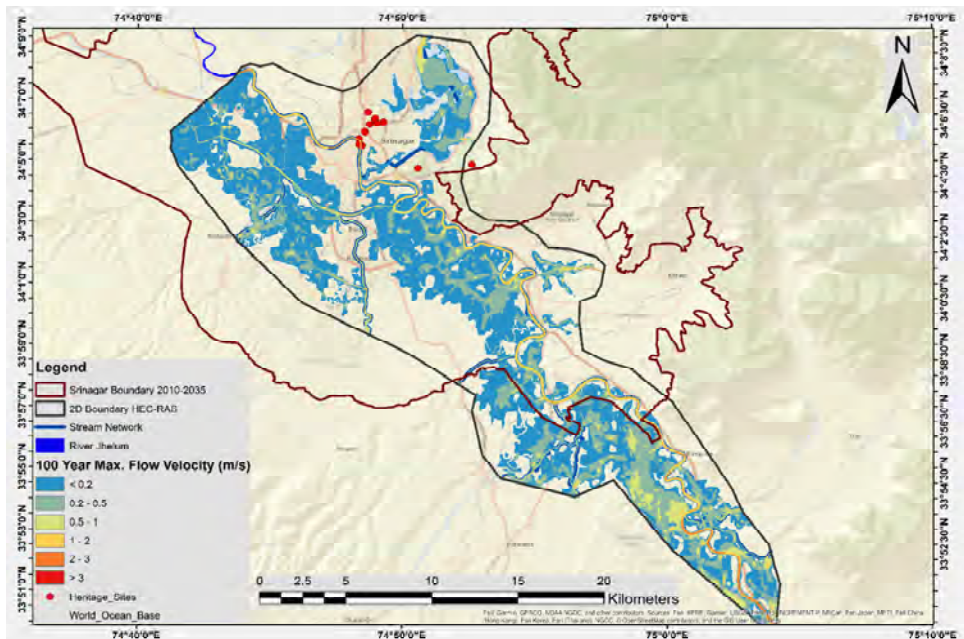


Figure 16 Maximum flow velocity of the 50-year flood (see online version for colours)

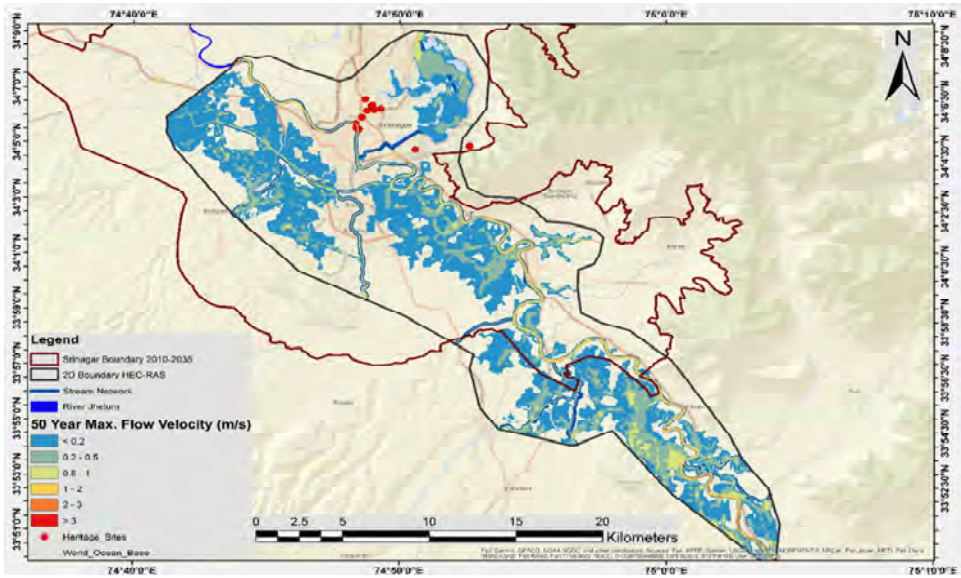


Figure 17 Maximum flow velocity of the 25- year flood (see online version for colours)

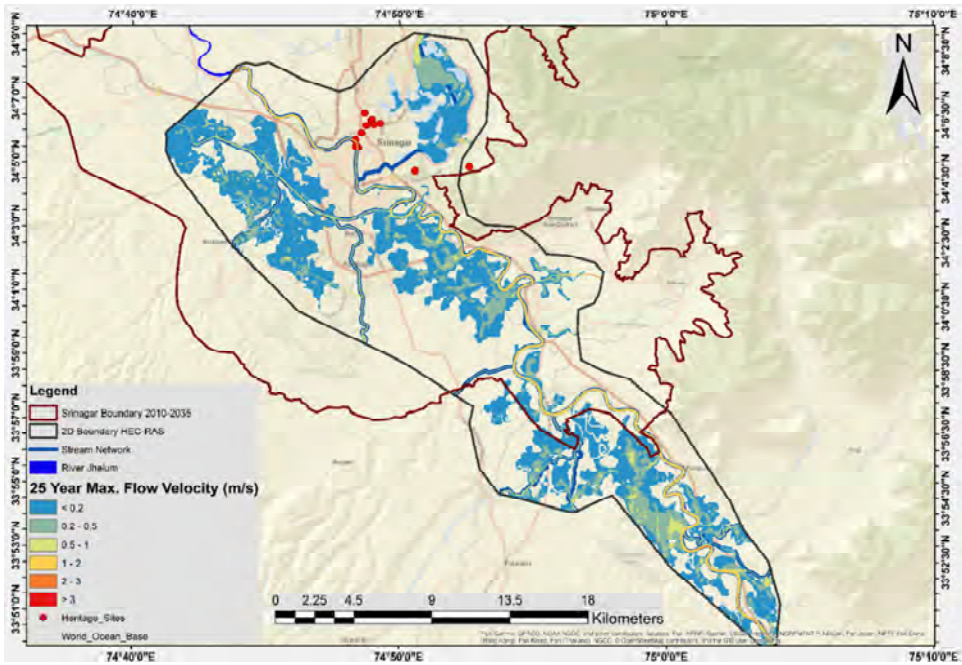
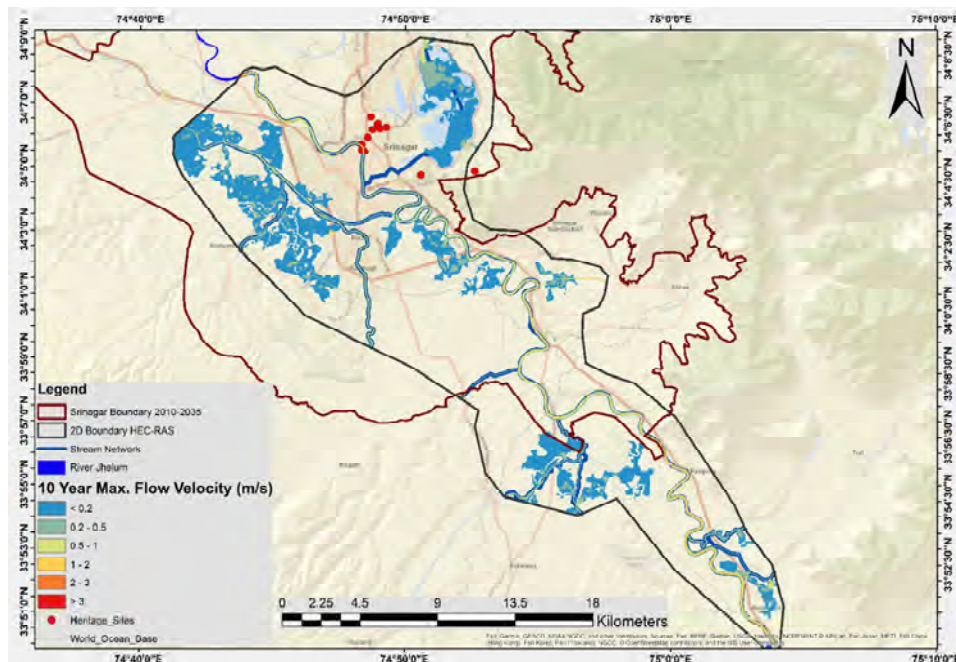


Figure 18 Maximum flow velocity of the 10-year flood (see online version for colours)

4 Conclusions

This study intends to assess the potential impact of the floods using unsteady state 2D flood modelling and mark the flood flow routes and flood levels from Sangam to Srinagar, including a significant portion of the Greater Srinagar (Plan 2010–2035) shown in all the inundation maps for different scenarios. This task is taken up so that adaptation measures can be taken before facing eventualities. All the softwares show efficient and encouraging results whether used for data processing or predicting the flooding extent. The risk of flooding is noticeable in the flood inundation maps. Because of this, it has become essential to create awareness among the masses in flood-prone areas to understand the severity of events because of climate change and hence the vulnerability of building structures in the high flood depth zones.

The main scope of this study can be broken down into:

- Mapping catchment boundaries and watercourses using GIS and WMS software with the best representing refined DEM and an initial assessment performed on data quality and completeness of data acquired. This process achieved in WMS is an alternative approach used in the study to the use of HEC-GeoHMS. Finer resolution data can be used for improving the accuracy by the government-run agencies where fund availability is not a constraint.
- Preparation of the hydrological study for a 5, 10, 25, 50, 100-years design storm, incorporating existing information through freely available open-source software's WMS, HEC-HMS, and GIS tools to analyse the terrain and validate the

physiography of the catchment areas. This is the first study conducted in the Jhelum basin for the hypothetical storm estimation using rainfall data in HEC-HMS.

- Establishing the baseline flood risk to the Srinagar City from overland flow. Srinagar City flood maps and other readily available information estimate whether the areas around the mega river are at risk of flooding. Local overland flow routes were estimated using available best-suited DEM, and flow rates were calculated using standard methods such as the SCS method. The authors believe this is the first time a 2D unsteady state analysis has been conducted in the Jhelum River basin.
- Hydraulic modelling to identify and categorise areas where flooding may occur. The spatial expansion and the settlement plan of Srinagar City a significant concern as the studies make it evident that the wetlands and flood absorption zones have already become the hotspots of urbanisation and development. The study outlined the possible regions which could be referred to for constructing the buildings away from flood flow routes (Figures 11–13). This study aimed at categorising the inundated areas into flood risk zones for every design flood for each recurrence interval as very low, low, medium, high, and very high-risk. The results show that most of the land and developments on the left side of the River Jhelum were inundated in the 25-year, 50-year, and 100-year design floods. Appropriate measures need to be taken to safeguard lives and property. Three heritage sites marked in all the inundation maps were seen to be affected in the city. A provision of $\pm 10\%$ to the spatial extent of floods should be allowed in case of applying the results demarcated by the HEC-RAS model in the flooded regions as shown in simulations to safeguard the population and assets even though our results are very close to observations.

Immediate response strategies must be undertaken to prepare for events of the observed magnitude. Ground re-profiling to direct water away from buildings in the influence zone can be done. Sustainable drainage systems to ensure that flood risk is not increased can be installed according to the results obtained in the design flood maps. The revised drainage system is a need of the hour so that during events of increased overland flow, the water can be carried efficiently. Future work can be conducted using the gridded data to analyse and estimate future scenarios in the study area.

Availability of data and material

The datasets used for the study are available from the India Meteorological Department, Srinagar, India, and from the authors with the permission of the said department.

Acknowledgements

Saika Manzoor conceived of the presented idea and contributed to the work's implementation and analysis. Manzoor Ahmad Ahangar supervised the work and approved the manuscript.

The research is funded by MHRD, the Government of India.

References

- Aasim, M. et al. (2014) 'Geospatial monitoring of forests a case study of pirpanjal forest division, J&K', *International Journal of Remote Sensing & Geoscience (IJRSG)*, Vol. 3, No. 3, p.16 [online] www.ijrsg.com (accessed 30 January 2022).
- Abdessamed, D. and Abderrazak, B. (2019) 'Coupling HEC-RAS and HEC-HMS in rainfall-runoff modeling and evaluating floodplain inundation maps in arid environments: case study of Ain Sefra City, Ksour Mountain. SW of Algeria', *Environmental Earth Sciences*, Vol. 78, No. 19, DOI:10.1007/s12665-019-8604-6.
- Adhikari, P. et al. (2010) 'A digitized global flood inventory (1998–2008): compilation and preliminary results', *Natural Hazards*, Vol. 55, No. 2, pp.405–422, DOI: 10.1007/S11069-010-9537-2.
- Ahmad, T., Pandey, A.C. and Kumar, A. (2018) 'Flood hazard vulnerability assessment in Kashmir Valley, India using geospatial approach', *Physics and Chemistry of the Earth*, Vol. 105, pp.59–71, DOI:10.1016/J.PCE.2018.02.003.
- Alaghmand, S. et al. (2012) 'Comparison between capabilities of HEC-RAS and MIKE11 hydraulic models in river flood risk modeling (a case study of Sungai Kayu Ara River basin, Malaysia)', *International Journal of Hydrology Science and Technology*, Vol. 2, No. 3, pp.270–291, DOI:10.1504/IJHST.2012.049187.
- Aryal, D. et al. (2020) 'A model-based flood hazard mapping on the southern slope of Himalaya', *Water*, Vol. 12, No. 2, p.540, DOI:10.3390/W12020540.
- Ballesteros-Cánovas, J.A. et al. (2020) 'Recent flood hazards in Kashmir put into context with millennium-long historical and tree-ring records', *Science of the Total Environment*, Vol. 722, DOI:10.1016/j.scitotenv.2020.137875.
- Bhat, M.S. et al. (2019) 'Flood hazard assessment of the Kashmir Valley using historical hydrology', *Journal of Flood Risk Management*, Vol. 12, No. S1, DOI:10.1111/jfr3.12521.
- Boodhoo, Y. (2003) 'Our future climate', *World Meteorological Organization Bulletin*, Vol. 52, pp.224–2s28.
- Dawson, R.J. et al. (2009) 'Integrated analysis of risks of coastal flooding and cliff erosion under scenarios of long term change', *Climatic Change*, Vol. 95, No. 1, pp.249–288, DOI:10.1007/S10584-008-9532-8.
- Derdour, A., Bouanani, A. and Babahamed, K. (2017) 'Hydrological modeling in semi-arid region using HEC-HMS model. case study in Ain Sefra watershed, Ksour Mountains (SW-Algeria)', *Journal of Fundamental and Applied Sciences*, Vol. 9, No. 2, p.1027, DOI:10.4314/JFAS.V9I2.27.
- Dottori, F. et al. (2018) 'Increased human and economic losses from river flooding with anthropogenic warming', *Nature Climate Change*, Vol. 8, No. 9, pp.781–786, DOI:10.1038/s41558-018-0257-z.
- Floods (2019) [online] https://www.who.int/health-topics/floods#tab=tab_1 (accessed 29 January 2022).
- Ghanbarpour, M. et al. (2014) 'Floodplain inundation analysis combined with contingent valuation: implications for sustainable flood risk management', *Water Resources Management: An International Journal, Published for the European Water Resources Association (EWRA)*, Vol. 28, No. 9, pp.2491–2505, DOI:10.1007/S11269-014-0622-2.
- Hashemyan, F. et al. (2015) *Combination of HEC-HMS and HEC-RAS Models in GIS in Order to Simulate Flood (Case Study: Khoshke Rudan River in Fars Province, Iran)*, isca.me [online]. <http://www.isca.me/rjrs/archive/v4/i8/20.ISCA-RJRS-2014-42.pdf> (accessed 3 February 2022).
- Horritt, M.S. and Bates, P.D. (2002) 'Evaluation of 1D and 2-D numerical models for predicting river flood inundation', *Journal of Hydrology*, Vol. 268, Nos. 1–4, pp.87–99, DOI:10.1016/S0022-1694(02)00121-X.

- Karbasi, M., Shokoohi, A. and Saghafian, B. (2018) 'Loss of life estimation due to flash floods in residential areas using a regional model', *Water Resources Management*, Vol. 32, No. 14, pp.4575–4589, DOI:10.1007/S11269-018-2071-9.
- Koneti, S., Sunkara, S.L. and Roy, P.S. (2018) 'Hydrological modeling with respect to impact of land-use and land-cover change on the runoff dynamics in Godavari River Basin using the HEC-HMS model', *ISPRS International Journal of Geo-Information*, Vol. 7, No. 6, p.206, DOI:10.3390/IJGI7060206.
- Kumar, N. et al. (2019) 'Applicability of HEC-RAS 2-D and GFMS for flood extent mapping: a case study of Sangam area, Prayagraj, India', *Modeling Earth Systems and Environment*, Vol. 6, No. 1, pp.397–405, DOI:10.1007/S40808-019-00687-8.
- Kumar, R. and Acharya, P. (2016) 'Flood hazard and risk assessment of 2014 floods in Kashmir Valley: a space-based multisensor approach', *Natural Hazards*, Vol. 84, No. 1, pp.437–464, DOI:10.1007/S11069-016-2428-4/FIGURES/16.
- Lee, K.S. and Lee, S.I. (2003) 'Assessment of post-flooding conditions of rice fields with multi-temporal satellite SAR data', *International Journal of Remote Sensing*, Vol. 24, No. 17, pp.3457–3465, DOI:10.1080/0143116021000021206.
- Liu, Z., Merwade, V. and Jafarzadegan, K. (2019) 'Investigating the role of model structure and surface roughness in generating flood inundation extents using one-and two-dimensional hydraulic models', *Journal of Flood Risk Management*, Vol. 12, No. 1, p.e12347, DOI:10.1111/JFR3.12347.
- Madhuri, R. et al. (2021) 'Urban flood risk analysis of buildings using HEC-RAS 2-D in climate change framework', *H2Open Journal*, Vol. 4, No. 1, pp.262–275, DOI:10.2166/H2OJ.2021.111.
- Mukherjee, S. et al. (2018) *Increase in Extreme Precipitation Events Under Anthropogenic Warming in India*, Elsevier [online] <https://www.sciencedirect.com/science/article/pii/S2212094717301068> (accessed 31 January 2022).
- Muslim, M.U. et al. (2014) 'Dynamics and forecasting of population growth and urban expansion in Srinagar City – a geospatial approach monitoring the urban growth of Dhaka (Bangladesh) by satellite imagery in flooding risk management', *Dynamics and Forecasting of Population Growth and Urban Expansion in Srinagar City – A Geospatial Approach*. DOI:10.5194/isprsarchives-XL-8-709-2014.
- Nkwunonwo, U.C., Whitworth, M. and Baily, B. (2020) 'A review of the current status of flood modelling for urban flood risk management in the developing countries', *Scientific African*, Vol. 7, p.e00269, DOI:10.1016/J.SCIAF.2020.E00269.
- Pender, G. and Néelz, S. (2007) 'Use of computer models of flood inundation to facilitate communication in flood risk management', *Environmental Hazards*, Vol. 7, No. 2, pp.106–114, DOI:10.1016/J.ENVHAZ.2007.07.006.
- Prama, M. et al. (2020) 'Vulnerability assessment of flash floods in Wadi Dahab Basin, Egypt', *Environmental Earth Sciences*, Vol. 79, No. 5, pp.1–17, DOI:10.1007/S12665-020-8860-5/FIGURES/9.
- Quiroga, V.M. et al. (2017) 'Application of 2-D numerical simulation for the analysis of the February 2014 Bolivian Amazonia flood: application of the new HEC-RAS version 5', <http://dx.doi.org/10.1016/j.riba.2015.12.001>, Vol. 3, No. 1, pp.25–33, DOI:10.1016/J.RIBA.2015.12.001.
- Ray, K., Bhan, S.C. and Bandopadhyay, B.K. (2015) 'The catastrophe over Jammu and Kashmir in september 2014: A meteorological observational analysis', *Current Science*, Vol. 109, No. 3, pp.580–591 [online] <http://bhuvan-noeda.nrsc.gov.in/> (accessed 31 January 2022).
- Romshoo, S.A. et al. (2017) *Climatic, Geomorphic and Anthropogenic Drivers of the 2014 Extreme Flooding in the Jhelum Basin of Kashmir, India*, Vol. 9, No. 1, pp.224–248 [online] <http://www.tandfonline.com/action/journalInformation?show=aimsScope&journalCode=tgnh20#.VsXodSCLRhE>, DOI:10.1080/19475705.2017.1417332.

- Romshoo, S.A. et al. (2018) 'Climatic, geomorphic and anthropogenic drivers of the 2014 extreme flooding in the Jhelum basin of Kashmir, India', *Geomatics, Natural Hazards and Risk*, Vol. 9, No. 1, pp.224–248, DOI:10.1080/19475705.2017.1417332.
- Shah, A.A. and Malik, J.N. (2017) 'Four major unknown active faults identified, using satellite data, in India and Pakistan portions of NW Himalaya', *Natural Hazards*, Vol. 88, No. 3, pp. 845–1865, DOI:10.1007/S11069-017-2949-5.
- Shah, A.A. et al. (2018) 'Living with earthquake and flood hazards in Jammu and Kashmir, NW Himalaya', *Frontiers in Earth Science*, Vol. 6, p.179, DOI:10.3389/FEART.2018.00179/BIBTEX.
- Sharifi, F., Samadi, S.Z. and Wilson, C.A.M.E. (2012) 'Causes and consequences of recent floods in the Golestan catchments and Caspian Sea regions of Iran', *Natural Hazards*, Vol. 61, No. 2, pp.533–550, DOI:10.1007/s11069-011-9934-1.
- Smith, K. (2013) 'Environmental hazards: assessing risk and reducing disaster', *Environmental Hazards: Assessing Risk and Reducing Disaster*, pp.1–478, DOI:10.4324/9780203805305.
- Steffen, W. et al. (2017) *Cranking Up the Intensity : Climate Change And Extreme Weather Events*, Thank you for supporting the [online] <https://www.climatecouncil.org.au/uploads/1b331044fb03fd0997c4a4946705606b.pdf> (accessed 1 February 2022).
- Sunkpho, J. and Ootamakorn, C. (2011) 'Real-time flood monitoring and warning system', *Songklanakarin Journal of Science and Technology*, Vol. 33, No. 2, pp.227–235 [online] <http://rdo.psu.ac.th/sjstweb/index.php> (accessed 30 January 2022).
- Tabari, H. (2020) 'Climate change impact on flood and extreme precipitation increases with water availability', *Scientific Reports*, Vol. 10, No. 1, pp.1–10, DOI:10.1038/s41598-020-70816-2.
- Thakur, B. et al. (2017) *Coupling HEC-RAS and HEC-HMS in Precipitation Runoff Modelling and Evaluating Flood Plain Inundation Map*, pp.240–251 [online] https://digitalscholarship.unlv.edu/fac_articleshttps://digitalscholarship.unlv.edu/fac_articles/450 (accessed: 2 February 2022).
- Thanh Mai, D. and De Smedt, F. (2017) *A Combined Hydrological and Hydraulic Model for Flood Prediction in Vietnam Applied to the Huong River Basin as a Test Case Study*, DOI:10.3390/w9110879.
- Thirumurugan, P. and Krishnaveni, M. (2019) 'Flood hazard mapping using geospatial techniques and satellite images – a case study of coastal district of Tamil Nadu', *Environmental Monitoring and Assessment*, Vol. 191, No. 3, pp.1–17, DOI:10.1007/S10661-019-7327-1.
- Tullos, D. et al. (2016) 'Review of challenges of and practices for sustainable management of mountain flood hazards', *Natural Hazards*, Vol. 83, No. 3, pp.1763–1797, DOI:10.1007/S11069-016-2400-3.
- UCAR (2010) *Flash Flood Early Warning System Reference Guide, Flash Flood Early Warning System Reference Guide* [online] https://www.meted.ucar.edu/communities/hazwarnsys/haz_fflood.php.
- Wani, A.A. et al. (2016) 'Multi-temporal forest cover dynamics in Kashmir Himalayan region for assessing deforestation and forest degradation in the context of REDD+ policy', *Journal of Mountain Science*, Vol. 13, No. 8, pp.1431–1441, DOI:10.1007/S11629-015-3545-3.
- Xie, S.P. et al. (2015) 'Towards predictive understanding of regional climate change', *Nature Climate Change*, Vol. 5, No. 10, pp.921–930, DOI:10.1038/nclimate2689.
- Zhang, W. et al. (2014) *Modeling Sediment Transport and River Bed Evolution in River System*, undefined, pp.175–179. doi:10.7763/JOCET.2014.V2.117.

Appendix

Supplementary material

We selected the best distribution for each station based on the goodness of fit of the chosen distribution functions.

Srinagar

Model	Nb param.	XT	P(Mi)	P(Mi x)	BIC	AIC
Exponential (Maximum Likelihood)	2	160.234	14.29	70.36	439.908	436.084
Log-Pearson type 3 (Méthode SAM)	3	216.156	14.29	27.13	441.814	436.078
GEV (Maximum Likelihood)	3	268.303	14.29	2.51	446.571	440.835
Gumbel (Maximum Likelihood)	2	129.720	14.29	0.00	463.449	459.625
Gamma (Maximum Likelihood)	2	142.111	14.29	0.00	474.020	470.196
Weibull (Maximum Likelihood)	2	165.782	14.29	0.00	492.529	488.705
Pearson type 3 (Conditional maximum likeliho	3	212.338	14.29	N/D	N/D	N/D

Pahalgam

Model	Nb param.	XT	P(Mi)	P(Mi x)	BIC	AIC
Exponential (Maximum Likelihood)	2	188.428	14.29	40.86	356.965	353.638
Pearson type 3 (Maximum Likelihood)	3	165.165	14.29	25.57	357.902	352.912
Gumbel (Maximum Likelihood)	2	145.364	14.29	16.12	358.825	355.498
Gamma (Maximum Likelihood)	2	135.427	14.29	9.04	359.981	356.654
Log-Pearson type 3 (Méthode SAM)	3	150.605	14.29	3.62	361.813	356.822
GEV (Maximum Likelihood)	3	170.854	14.29	3.39	361.830	356.840
Weibull (Maximum Likelihood)	2	127.676	14.29	1.20	364.027	360.699

Gulmarg

Model	Nb param.	XT	P(Mi)	P(Mi x)	BIC	AIC
Gumbel (Maximum Likelihood)	2	138.041	14.29	57.72	456.754	452.970
GEV (Maximum Likelihood)	3	156.944	14.29	24.83	458.441	452.765
Log-Pearson type 3 (Méthode SAM)	3	162.461	14.29	10.02	460.255	454.580
Gamma (Maximum Likelihood)	2	137.326	14.29	7.39	460.864	457.080
Weibull (Maximum Likelihood)	2	143.538	14.29	0.03	472.061	468.278
Exponential (Maximum Likelihood)	2	216.156	14.29	0.01	475.425	471.641
Pearson type 3 (Conditional maximum likeliho	3	155.973	14.29	N/D	N/D	N/D

Qazigund

Model	Nb param.	XT	P(Mi)	P(Mi x)	BIC	AIC
Gumbel (Maximum Likelihood)	2	204.571	14.29	38.91	493.550	489.726
Gamma (Maximum Likelihood)	2	186.272	14.29	38.28	493.583	489.759
Pearson type 3 (Maximum Likelihood)	3	195.712	14.29	7.60	496.817	491.081
Log-Pearson type 3 (Méthode SAM)	3	195.787	14.29	6.54	497.117	491.381
GEV (Maximum Likelihood)	3	195.488	14.29	5.85	497.338	491.602
Weibull (Maximum Likelihood)	2	176.737	14.29	2.80	498.815	494.991
Exponential (Maximum Likelihood)	2	292.278	14.29	0.03	507.958	504.134

Kokernag

Model	Nb param.	XT	P(Mi)	P(Mi x)	BIC	AIC
Gumbel (Maximum Likelihood)	2	159.796	14.29	38.72	374.614	371.287
GEV (Maximum Likelihood)	3	195.525	14.29	22.23	375.724	370.733
Log-Pearson type 3 (Méthode SAM)	3	193.803	14.29	19.08	376.029	371.038
Pearson type 3 (Maximum Likelihood)	3	172.281	14.29	10.01	377.318	372.328
Gamma (Maximum Likelihood)	2	157.701	14.29	9.01	377.529	374.202
Exponential (Maximum Likelihood)	2	234.328	14.29	0.80	382.379	379.052
Weibull (Maximum Likelihood)	2	160.309	14.29	0.15	385.709	382.382

Kupwara

Model	Nb param.	XT	P(Mi)	P(Mi x)	BIC	AIC
Weibull (Maximum Likelihood)	2	95.005	14.29	46.07	361.455	357.980
Gamma (Maximum Likelihood)	2	104.953	14.29	21.21	363.007	359.532
Pearson type 3 (Maximum Likelihood)	3	96.433	14.29	19.19	363.207	357.994
GEV (Maximum Likelihood)	3	99.381	14.29	9.96	364.518	359.305
Gumbel (Maximum Likelihood)	2	125.743	14.29	3.56	366.574	363.098
Exponential (Maximum Likelihood)	2	215.205	14.29	0.00	408.773	405.297
Log-Pearson type 3 (Méthode SAM)	3	83.378	14.29	N/D	N/D	N/D